PCCP

Accepted Manuscript

ROYAL SOCIETY OF CHEMISTRY

www.rsc.org/pccp

Journal Name

ARTICLE

Carbazole-functionalzed Polyphenylene-decorated solid state emissive D-A-D molecules: Reduced Donor-Acceptor interaction and enhanced emission in solid state

Received 00th January 20xx,
Accepted 00th January 20xx

DOI: 10.1039/x0xx00000x

www.rsc.org/

Vandana Bhalla,* Gopal Singh and Manoj Kumar,*

A new series of D-A-D molecules (**1**-**3**) with carbazole as donor while 2,5-diaryl-1,3,4-oxadiazoles, dibenzothiophene-S,S-dioxide and Benzo[1,2,5] thiadiazole as acceptors have been synthesized. Polyphenylene dendrons have also been incorporated to prevent the face to face π–π stacking in aggregates. Unlike traditional D−A systems, which show ACQ problem and large red shifts in solid state, these derivatives (**1**-**3**) exhibit good solid state luminescence behavior without undergoing red shift or fluorescence quenching. The present results indicate that just the combination of donors-acceptor system with bulkier dendrons is not enough to generate efficient solid state emissions but prevention of co-facial interaction of donor and acceptors in aggregates is more important. In case of derivative **3**, restriction of complete molecular planarization and steric hindrance near acceptor can effectively prevent intermolecular donor acceptor interactions, thus, leading to enhanced emission in aggregates. While in case of derivative **1**, sterically unhindered acceptor is easily approached by donor due to close molecular packing in aggregates forming weakly luminescent species.

Introduction

Organic solid-state luminescent materials based on donor–acceptor (D–A) systems have gained increasing attention in recent years due to their potential applications in large-area flexible display, solid-state lighting, organic lasers etc owing to high fluorescent quantum yields and impressive bipolar charge-transporting properties.[1-3] Their intramolecular charge transfer (ICT) characteristic endows them with tunable electronic states which can be modulated by independent and diverse selection of donor and acceptor groups, making them suitable for wide variety of applications biophotonics and optoelectronics. These systems are anticipated to simplify the device configuration by reducing the number of active layers and consequently improving the device performance.[4-13] However, most of the conjugated D-A molecules show very high luminescence efficiency in dilute solutions only, and exhibit large bathochromic shift with relatively weak or no emissions in thin film due to aggregation caused quenching (ACQ) effect. This ACQ may be attributed to the facilitated non radiative decay induced by strong intermolecular interactions, including exciton coupling and excimer formation.[14] This ACQ is also responsible for reduced photoluminescence (PL) efficiency of these luminescent materials in the solid state and thus considered as a great obstacle towards the development of efficient optoelectronic devices using organic luminescent materials. The major challenge in developing luminescent materials with D–A systems is to prevent the large red shift in emission and ACQ in solid state while preserving the merits of the D–A architecture.[15-19,6] However, it is very hard to get higher solid-state efficiencies than those of molecularly dissolved species in non polar solvents.[20-21] Many methods have been adopted to reduce ACQ like doping method, introduction of π spacer, using weak π donor/weak π acceptor etc but they have met with limited success only.[22-25,6] Recently, the phenomena of aggregation-induced emission (AIE)[26] and aggregation-induced emission enhancement (AIEE)[27] have been found to be very effective to obtain highly emissive materials in solid state.[28-31] However, there are few reports in literature in which AIE has been used to obtain high solid-state efficiency in D–A molecules.[32-37] The current research on organic fluorescent materials indicates that the key point for designing high efficiency solid state luminescent materials is to suitably control the molecular orientations and stacking modes of fluorophores in aggregate form.

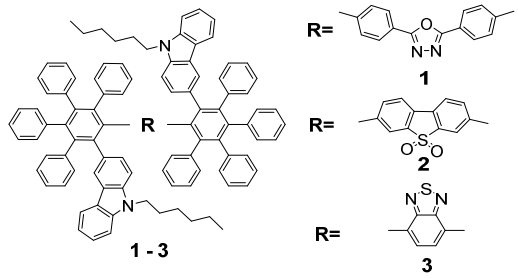

Fig. 1 Derivative **1-3**

Department of Chemistry, UGC Sponsored-Centre for Advanced Studies-I, Guru Nanak Dev University, Amritsar-143005, Punjab, India.
E-mail: vanmanan@yahoo.co.in ; mksharmaa@yahoo.co.in; Fax: +91 (0)183 2258820; Tel: +91 (0)183 2258802-9 ext. 3202, 3205
Electronic Supplementary Information (ESI) available: See
DOI: 10.1039/x0xx00000x

Keeping in mind the importance of D-A systems, we planned to design and synthesize D-A-D molecules (**1**-**3**) with carbazole substituted polyphenylene as donor and 2,5-diaryl-1,3,4-oxadiazoles/ dibenzothiophene-S,S-dioxide/ Benzo[1,2,5] thiadiazole as acceptor, respectively. Carbazole is known for its thermal stability and good hole-transporting ability.[38-39] On the other hand, 2,5-diaryl-1,3,4-oxadiazoles,[40-41] dibenzothiophene -S,S-dioxide[42-44] and benzo[1,2,5 thiadiazole[45] are versatile electron-transporting materials with high electron affinity. We incorporated non planar polyphenylene aromatic units into the molecule. We expected that these units will provide good thermal and morphological stability to the molecule and will prevent aggregation caused quenching by reducing Intermolecular π–π interactions of donor and acceptor in solid state[46-48] and could lead to formation of luminescent D-A materials. The results of our investigation show that reduction in size of acceptor lead to increase in steric hindrance and reduced intermolecular donor-acceptor interaction in case of derivative **2** and **3** which resulted in their efficient emission in aggregate state. On the other hand, in case of derivatives **1** relatively unhindered acceptor is easily approached by the donor in aggregates and quenching of emission is observed. The photophysical, electrochemical, thermal and morphological properties of these derivatives are investigated in detail to elucidate the mechanism of enhanced emission in the aggregate state.

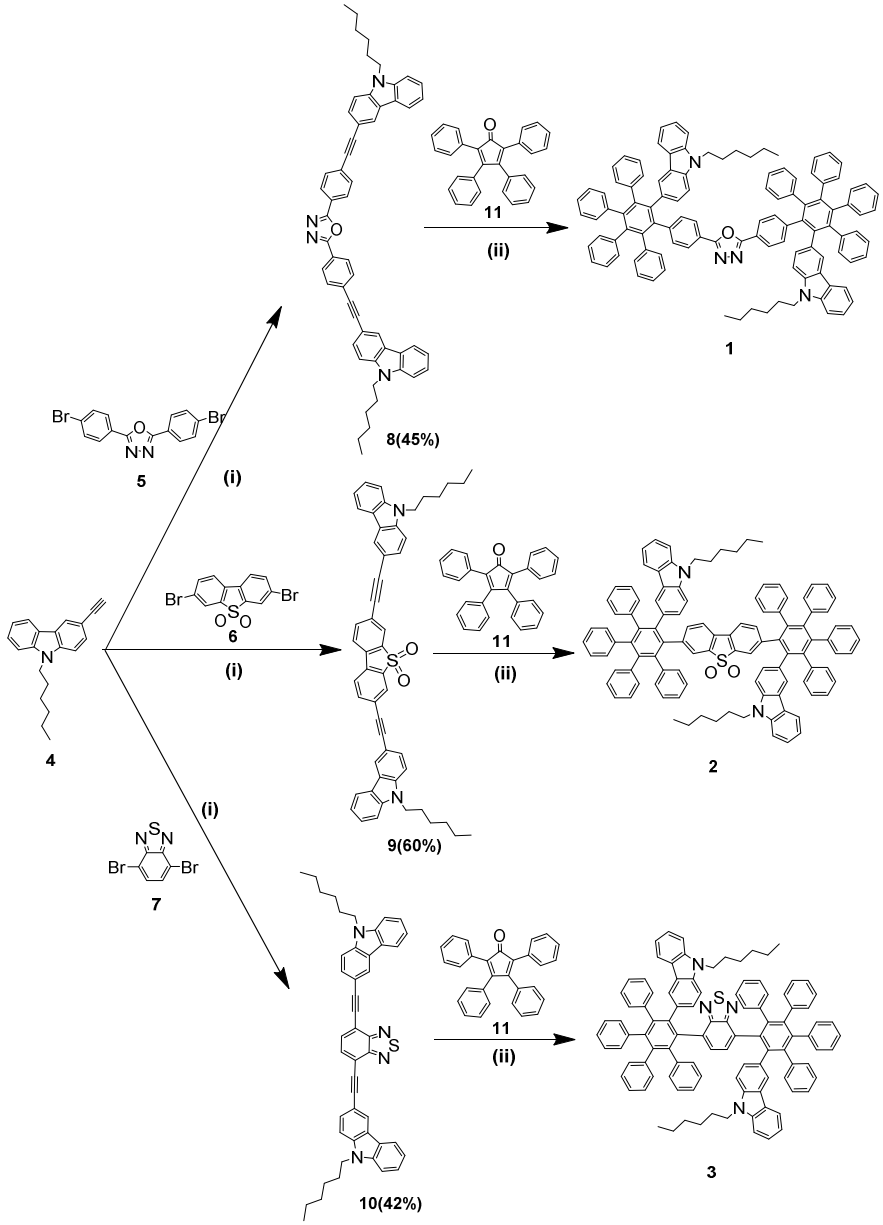

Scheme 1. Synthesis of derivative **1-3:** Reaction conditions: (I) $Pd(PPh_3)_4$, CuI, TEA,toluene, 75 °C, 24 h; (II) Ph_2O, reflux, 48h.

Results and Discussion

The precursors **4**,[49] **5**[50] and **6**[51] were synthesised by following the already reported procedure in the literature. Sonogashira cross coupling of precursor **4** with **5**, **6** and **7** in the presence of palladium catalyst and copper Iodide as co-catalyst gave the compounds **8**, **9** and **10**, respectively. Further, the Diels Alder reaction of **8**, **9** and **10** with **11** furnished the target molecules **1**, **2** and **3** in 25%, 37% and 39% yield, respectively. The structures of these derivatives were confirmed by NMR and mass spectroscopy. Mass spectra of derivative **1**, **2** and **3** showed molecular ion peaks at *m/z* 1481.68, 1475.57 and 1395.65, respectively which corroborate with the structure of these derivatives.

Thermal Properties

To explore the thermal properties of the derivatives, thermal gravimetric analysis (TGA) and differential scanning colorimetric (DSC) measurements were performed at a scanning rate of 10 ºC min^{-1} under flowing nitrogen. As shown in Fig. 2, TGA curve reveals very high decomposition temperature, T_d ($T_{d5\%}$, corresponding to 5% weight loss) at 410, 385 and 378 ºC for derivative **1**, **2** and **3** respectively, which indicate their high thermal stability. High thermal stability is highly desirable to improve the efficiency and lifetime of organic electronic devices. DSC curve exhibit only an endothermic baseline shift due to glass transitions (T_g) at 181 and 243 ºC for derivative **1** and **3,** respectively, while no T_g baseline shift could be observed for **3** (See Fig. S1, ESI). We believe that the presence of bulky aryl groups is responsible for their high thermal stability.

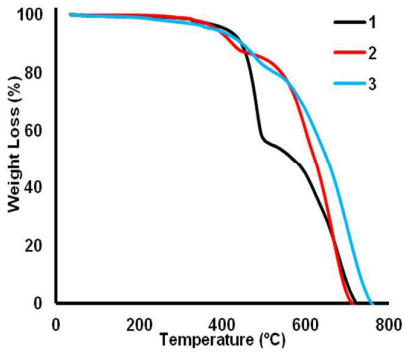

Fig. 2 TGA curves of derivative **1-3**

Electrochemical Properties

Cyclic voltammetry studies were carried out to reveal the electrochemical behaviour of these compounds. All the derivatives exhibited single oxidation peak with irreversible electrochemical behaviour which was assigned to oxidation of the carbazole (Fig. 3). Irreversible behaviour is due to the intermolecular cross linking of the carbazole radical intermediate via the free 3 and 6 positions of the carbazole moiety.[52]

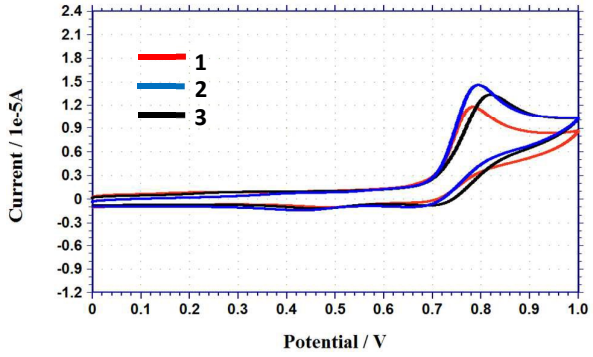

Fig. 3 Cyclic voltamograms of derivative **1-3.**

The whole data is summarized in table 1. HOMO and LUMO energy levels were calculated from the oxidation onset potentials (E_{onset}) and energy gaps (E_g). On the basis of the onset oxidation potential, we estimated the HOMO energy levels of derivative with regard to ferrocene (-4.8 eV below vacuum),[53] which was found to be -5.50 eV, -5.51 eV and -5.51 eV for derivative **1**, **2** and **3**, respectively. The optical band gaps were determined by the absorption edge technique.[54]Accordingly, the LUMO energy levels were also calculated by subtracting the band gap of these derivatives from the HOMO energy level of these derivatives. It is clear from the electrochemical data that HOMO levels are almost same for all three derivatives while LUMO levels have shown considerable change due to differences in the electron affinities of acceptor groups. High lying HOMO and low lying LUMO levels would facilitate hole and electron injection in electronic devices, respectively. Repeated cycles show slight decrease in current which suggests electrochemical oxidative coupling reaction at the 3,6 positions of carbazole leading to electro-polymerization and its deposition on working electrode (See Fig. S2-S4, ESI).

Table 1. Electrochemical and thermal properties of derivative **1-3**

Comp.	$T_g/T_m/T_d$ °C	HOMO/LUMO eV	Band Gap eV
1	181/324/410	-5.5/-2.14	3.36
2	ND/ND/385	-5.51/-2.26	3.25
3	243/ND/378	-5.51/-2.62	2.89

Theoretical calculations

To understand the geometry and electronic structures of derivatives **1**-**3**, density functional theory (DFT) calculations were performed with B3LYP/6-31G basic set using the Gaussian 09 program. The optimized ground-state structures of the derivatives **1**-**3** are shown in Figure 4. The ground state optimized structures revealed that all the derivatives possess twisted spatial conformations. The dihedral angles of the acceptor core and the peripheral polyphenylene (PP) groups

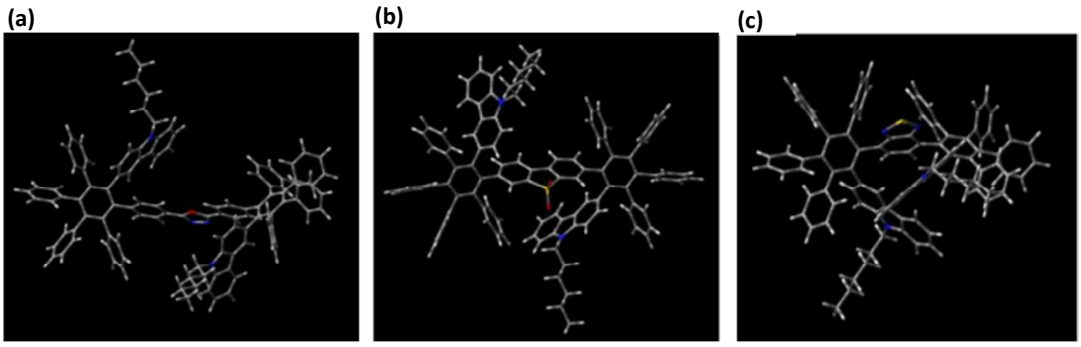

Fig. 4. Optimized ground state strucures of derivative **1** (a), **2** (b) and **3** (c)

are in the range from 56 to 72º. For derivative **1**, the dihedral angle between the acceptor and both PP units is 66.2º while carbazole units are twisted out of plane from central benzene ring of PP unit at 67.1º angle. For derivative **2**, both PP units are aligned at slightly different angles (64.6 and 66º) with respect to acceptor core while carbazole units are twisted out of plane from central benzene ring at 66.09 and 72.6º. In case of derivative **3** both PP units are aligned at 63 and 56.2º with respect to acceptor core while carbazole units are twisted out of plane from central benzene ring at 66.1 and 71º. Phenyl rings of PP groups are twisted out of plane from central benzene ring with dihedral angle from 58 to 68º. These twisted conformations hamper the π-π stacking interactions between the molecules and enable them to emit efficiently in solid state. Higher steric congestion is observed near acceptor core in case of derivative **3** as compared to derivatives **1** and **2**.

Photophysical Properties

Photophysical properties of derivatives **1**-**3** were investigated by UV-visible absorption and fluorescence spectroscopy. All the derivatives are freely soluble in most of the common organic solvent due to the presence of alkyl chains on carbazole. The absorption spectra of derivatives **1**-**3** reveal an absorption band located around 300 nm due to π-π* electronic transitions of the carbazole[55] and a shoulder around 355 nm due to π-π* electronic transitions of conjugated backbone (Fig. 5). Among all the three derivatives, **3** having benzothiadiazole as acceptor exhibited absorption and emission at longer wavelength. This result is in accordance with the lowest LUMO energy calculated in case of derivative **3**.[45]

Solvatochromism

The absorption and emission behaviors of all the three derivatives were explored using different solvents with a wide range of polarity (Table 2). The details of absorption, emission and time resolved spectra recorded in different solvents of varying polarity and thin film are summarized in table 2. The absorption and fluorescence spectra of thin film were recorded by drop casting DCM solution of the derivatives on a quartz substrate. When going from toluene to DMSO, the absorption spectra of these derivatives scarcely changed, thus, indicating very stable ground state and negligible intramolecular charge transfer process between donor and acceptor in the ground state (Fig. 6). In sharp contrast to the minor solvent dependent absorption spectral features, the emission spectra of these molecules exhibited a prominent positive solvatochromic effect indicative of great dipole moment in the excited state (Fig. 6). All the three derivatives showed bathochromic shifts in the emission maximum upon increasing the solvent polarity. The main emission peaks changed from 416 nm in toluene to 471 nm in DMSO for **1**, from 443 nm in toluene to 499 nm in DMSO for **2** and from 480 nm in toluene to 550 nm in DMSO for **3** (Table 2), suggesting

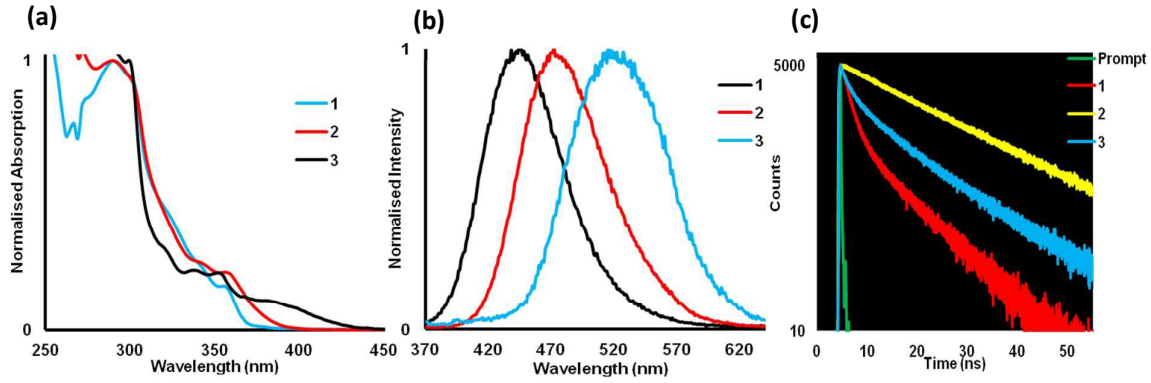

Fig. 5. UV-visible (a), fluorescence (b) and time resolved spectra (c) of derivative **1**-**3** in DCM (conc. - 10μM, λex = 355 nm for **1** and **2** and 352 nm for **3**).

Table 2. Photophysical and decay properties of derivative **1-3**

Comp.		Absorption (λ_{max}) (nm)	Emission (λ_{max}) (nm)	QY Φ_F	τ_1[a](A)[b] (ns)	τ_2[a](A)[b] (ns)	τ_F[c] (ns)
1	Tol.	290, 355	416	0.46	1.14(64%)	4.39(36%)	1.55
	THF	290, 355	433	0.46	1.41(55%)	6.25(45%)	2.18
	DCM	290, 355	444	0.63	1.78(48%)	9.18(52%)	3.06
	DMSO	290, 355	471	0.55	2.74(31%)	19.5(69%)	6.74
	Thin film	290, 356	445	-	0.76(63%)	3.46(37%)	1.07
2	Tol.	290, 355	443	0.43	3.43(11%)	7.41(89%)	6.57
	THF	290, 355	461	0.40	5.09(3%)	12.2(97%)	10.81
	DCM	290, 355	472	0.47	6.13(0.4%)	16.6(99.6%)	16.5
	DMSO	290, 355	499	0.32	0.85(0.55%)	29.7(99.45%)	25.10
	Thin film	292, 352	450		2.61(41%)	8.30(59%)	4.37
3	Tol.	299, 352	480	0.1	2.55(24%)	9.50(76%)	5.71
	THF	299, 352	493	0.03	1.64(21%)	8.77(79%)	4.49
	DCM	299, 352	515	0.02	2.14(19%)	12.3(81%)	6.41
	DMSO	299, 352	550	0.01	2.98(14%)	13.5(86%)	9.01
	Thin film	299, 352	478	-	3.32(30%)	10.0(70%)	6.21

a = fluorescence life time, b = percent contribution, c = weighted mean life time

typical ICT emissions for these compounds in solution.[56-59]

We believe that derivatives **1** and **2** are emissive in their solutions due to conformational stiffness and planarity in the excited state owing to small steric effects.[60-61] The fluorescence quantum yields of **1** and **2** increases from 47 and 43% in non polar toluene to 63 and 47% in medium polarity DCM, respectively, indicating better stabilization of the highly polar emitting state by polar solvents however, quantum yield decrease in highly polar DMSO to 55 and 32% respectively, which is a common property of molecules exhibiting large charge separation in the excited state. Further, a significant decrease in quantum yield of derivative **2** in DMSO is observed which may be attributed to the partial twisting of donor acceptor units in excited state due to high polarity. On the other hand, derivative **3** was found to be weakly emissive in solution. We believe that the out of plane twisting of carbazole units in excited state owing to steric congestion near smaller sized benzothiadiazole makes it more susceptible to non radiative decay, resulting in a weaker emission in solution.[56]Further emission studies of derivative **3** showed gradual decrease in quantum yield on increasing the polarity of solvents (0.1, 0.03, 0.02 and 0.01 in toluene, THF, DCM and DMSO, respectively). Red shifted emission along with decrease in quantum yield with increasing solvent polarity indicates the presence of twisted intramolecular charge transfer (TICT) which is usually observed in D-A systems.[29,57,62-64] TICT weakens the fluorescence due to its susceptibility towards non radiative decay quenching process.

To examine the presence of TICT in derivatives **1**-**3**, we carried out temperature dependent fluorescence studies as it is well known that TICT emission is sensitive to temperature variation.[65] Gradual increase in fluorescence intensity accompanied by blue shifting of emission maxima with increasing temperature was observed which confirms the presence of TICT in case of derivative **2** and **3** (Fig. 7). On the other hand, very small increment of fluorescence intensity and blue shift was observed in derivative **1** which shows absence of TICT state in case of derivative **1.**

Time-resolved fluorescence measurements of derivative **1**-**3** were also performed and the detailed data of these studies are listed in table 2. The fluorescence decay behavior of all the three derivatives **1**-**3** in different solvents and thin film is well-fitted by the double-exponential. All the derivatives have shown longer life time with increasing solvent polarity which shows better stabilization of excited state in polar solvents (Fig. 6). Excited states of **1**-**3** decay via fast and slow channels. With increase in solvent polarity, decay via fast channel is slowed while decay via slow channel is populated which is consistent with increased life time of **1**-**3** with solvent polarity. Derivative **2** exhibits longest fluorescence life times which may be attributed to the larger delocalization of electrons in this case which leads to a larger molecular stabilization effect for the excited state. Furthermore, the derivatives **1**-**3** also exhibited good thin film photoluminescence (PL) behaviour. This is expected due to the molecular design because sterically crowded polyphenylene prevent molecular aggregation consequently inhibiting ACQ. Except derivative **1**, photoluminescence spectra of the materials in thin films are almost similar to their spectra in nonpolar toluene solution (Figure 6), thus, indicating that the aggregation is suppressed. The derivative **1** emits at 445 nm in thin film, about 29 nm red-shifted from that of its toluene solution (416 nm) while derivatives **2** and **3** have emission at 450 and 480 nm in thin film and 443 and 480 nm in toluene, respectively. This shows that the emissive species for **1**, in aggregated state is different from those in solution which is further supported by PL decay dynamics (vide infra). A

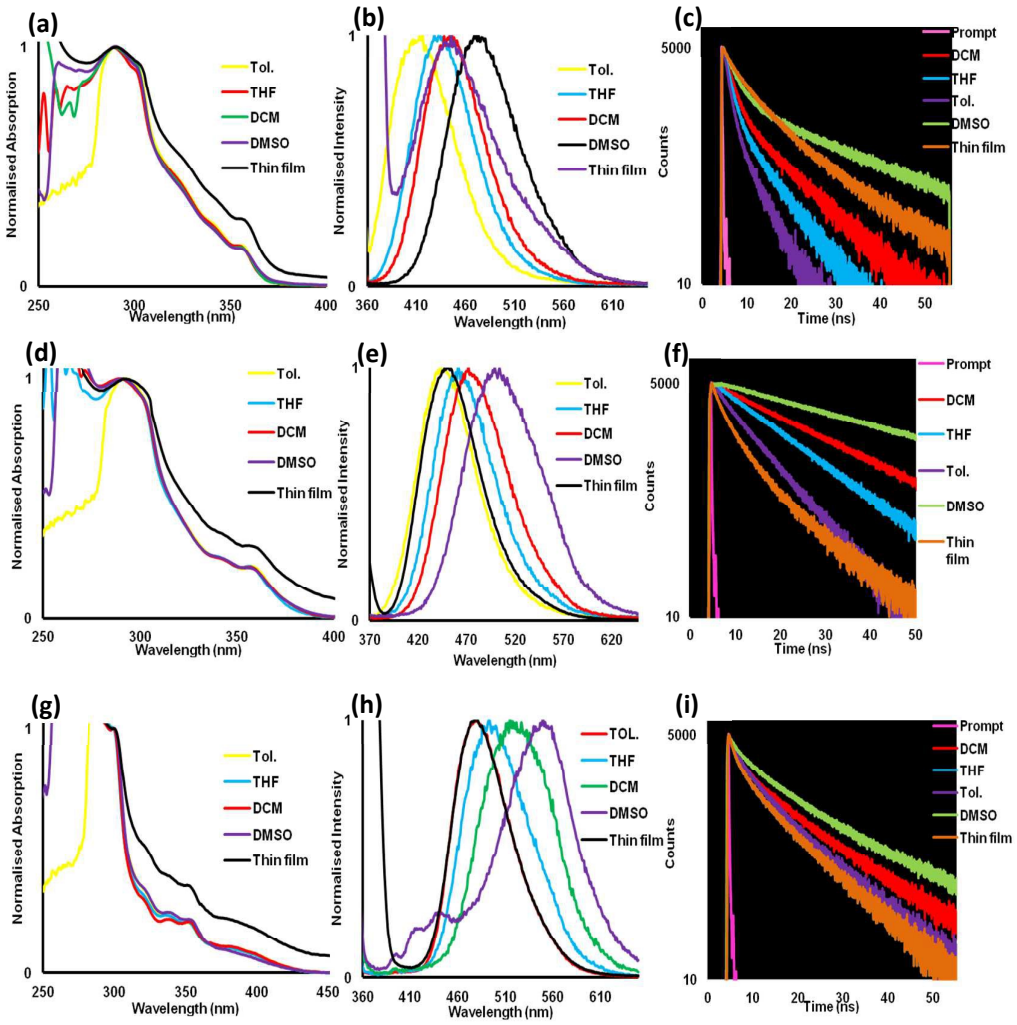

Fig. 6 UV-visible (a, d, g), fluorescence (b, e, h) and time resolved spectra (c, f, i) of derivative **1**, **2** and **3** respectively.

considerably faster excited state decay of derivative **1** in neat film (1.07 ns) indicated enhanced excitation migration and non-radiative relaxation at the quenching sites.

ACQ to AIE

Organic molecules with propeller shaped structure or with rotatory groups are known to show aggregation induced emission (AIE) or aggregation induced emission enhancement (AIEE) effect.[60] The presence of phenyl rotors in derivatives **1**-**3** prompted us to explore AIE(E) characteristics of these molecules, thus, we carried out aggregation studies of these derivatives in THF/water solvent mixture. Despite structural similarity, these derivatives exhibited very different aggregation behavior. Only derivatives **2** and **3** were found to be AIE active while derivative **1** displayed ACQ.

The absorption spectra of all derivatives (**1**-**3**) exhibited no spectral shift in presence of water fractions ranging from 0% to 50%, which is similar to their behavior in different solvent (As the solvent polarity increases with addition of water).[66] However, when water fraction is further increased (60-90%), leveling off tail appears in the visible region of spectra due to the formation of aggregates (Mie scattering effect).[67] Further the absorption spectra of the aggregates formed at the water fraction of 90% were found to be same as that of their thin film absorption (See Fig. S5-S7, ESI). In the fluorescence studies of derivatives **1-3**, the emission peaks of all derivatives are red-shifted with gradual addition of water upto 50% (Fig. 8, 9 and 10). We believe that the red shifting of emission band in presence of 50% water fraction is due to solvent polarity effect.[64] However, when water fraction was increased from 60% to 90%, emission maximum was blue-shifted due to elimination of solvent polarity effect in the aggregates.[68] This blue shift emission upon aggregation is common behavior in all the three derivatives (Table 3).

The fluorescence studies of derivative **1** showed small enhancement in emission intensity with increase in water fraction upto 50% which is due to better stabilization of its charge transfer state in more polar solvents (vide supra).

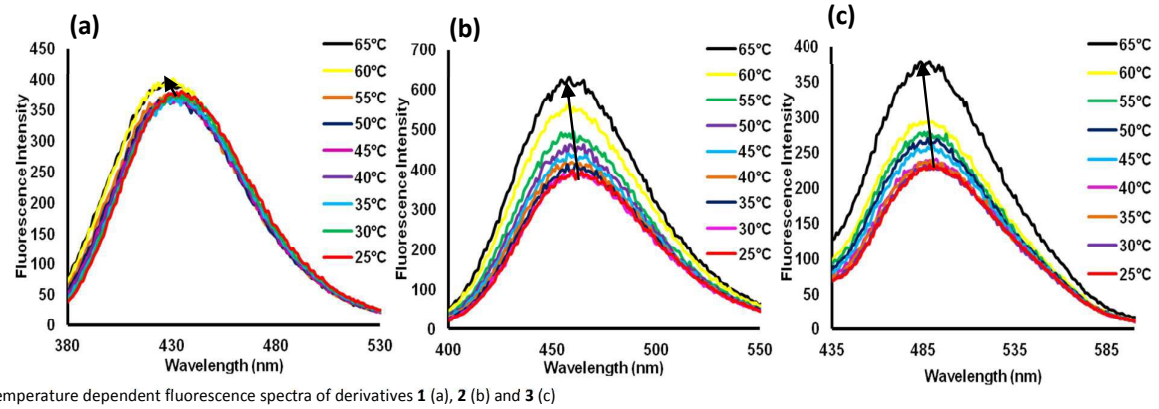

Fig. 7 Temperature dependent fluorescence spectra of derivatives **1** (a), **2** (b) and **3** (c) in THF. {Slit width used – 3:1.5 for derivative **1** and **2** while 3:3 for derivative **3}**.

However, upon further increasing the water fraction from 60% to 90%, a decrease in emission intensity is observed due to intermolecular interactions in aggregates. The donor carbazole can easily approach less sterically hindered oxadiazole acceptor of neighbouring molecule, forming intermolecular charge transfer state, which reduces the emission intensity of aggregates.[69-70] DLS studies show reduction in particle size of aggregates upon increasing water fraction from 600-1400nm in 60% to 30-140nm in 90% water (See Fig. S17 and S18, ESI). Fluorescence life time of derivative also increased with increasing water content due to stabilization of charge but decreased sharply with the formation of aggregates which is consistent with fluorescence studies.[71] Tri exponential decay of aggregates also indicates the formation of additional non radiative decay pathway in aggregates.

Morphological investigation of the aggregates by transmission electron microscope (TEM) image and electron diffraction spectroscopy (ED) spectrum indicates that the aggregates formed in 60% and 90% (fw) mixture are round in shape with amorphous state and give an obscure diffuse halo in ED spectrum (See Fig. S11 and S12, ESI). Amorphous nature of derivative **1** is also confirmed by powder XRD analysis (See Fig. S8, ESI) which showed no sharp peaks.

Derivative **2** exhibited red shifting of emission band along with decrease in emission intensity when the water fraction in the THF/water mixtures is increased from 0 to 50%, however, in presence of 60% water fraction, a blue shift along with emission enhancement is observed and emission intensity reaches same as that in pure THF (Φ=0.40). But it again decreases in 80 and 90% water (Table 3). This phenomenon may be attributed to the formation of crystalline or amorphous particles. Crystalline particles leads to enhancement while amorphous leads to reduction in emission intensity.[72]

TEM images show formation of nano rods in 60% water fraction with clear diffraction spots in ED spectra which confirm the crystalline nature of aggregates (See Fig. S13, ESI), while in 90% water only amorphous spherical aggregates are observed giving only an obscure diffuse halo in ED spectra (See Fig. S14, ESI). Powder-XRD patterns also show many sharp peaks indicating degree of order present in powder sample (See Fig. S9, ESI). In higher water content (90%) the molecules are more tightly packed into aggregates leading to stronger intermolecular interactions, thus, reducing the emission intensity. This behavior is consistent with decrease in fluorescence life time of aggregates in 90% water fraction as compared to 60% (Table 3). The lifetime of **2** is almost from the contribution of the longer lifetime species in solution, while in aggregates the contribution of shorter lifetime species is increased. DLS studies also show that the average particle size decreases from 600-1200 nm in 60% to 50-140nm in 90% water (See Fig. S19 and S20, ESI).

In case of derivative **3**, with gradual addition of water into THF

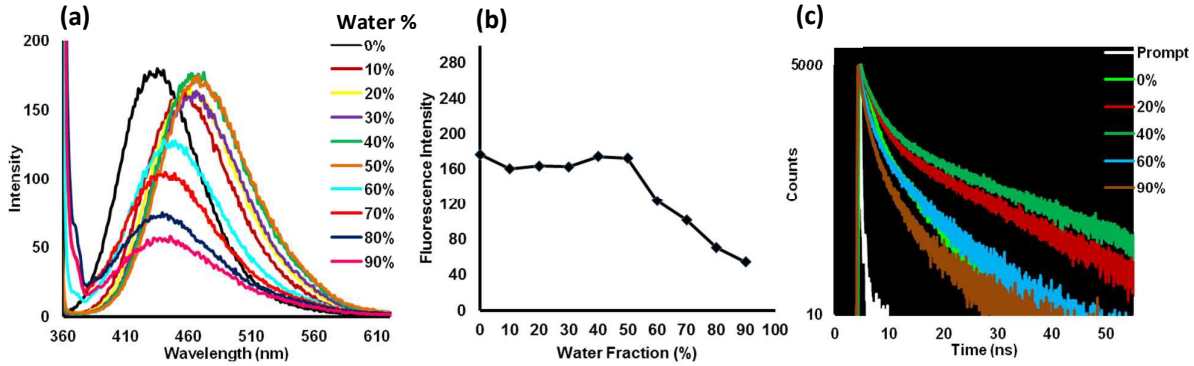

Fig. 8 Fluorescence spectra (a), fluorescence intensity (b) and time resolved spectra (c) of derivative **1** in THF with different water fractions. [slit width used – 3:1.5]

Table 3. Photophysical and decay properties of derivative **1-3** in different water fractions

	Water Fraction (%)	Emission λ_{max}(nm)	$\tau_1^a(A_1)^b$ (ns)	$\tau_2^a(A_2)^b$ (ns)	$\tau_3^a(A_3)^b$ (ns)	$<\tau>^c$ (ns)
1	0	435	1.54(56%)	6.36(44%)		2.32
	20	460	2.02(41%)	13.4(59%)		4.08
	40	468	2.19(35%)	15.5(65%)		4.91
	60	448	2.08(40%)	0.59(17%)	8.13(43%)	1.86
	90	435	1.73(56%)	0.34(17%)	7.66(27%)	1.18
2	0	466	0.43(0.4%)	11.6(99.6%)		10.66
	20	482	0.17(0.4%)	16.80(99.6%)		12.36
	40	487	0.35(0.7%)	16.80(99.3%)		12.67
	60	465	2.40(9%)	13.8(91%)		9.72
	90	446	3.67(35%)	11.4(65%)		6.60
3	0	490	2.20(20%)	8.95(80%)		5.59
	20	519	2.29(20%)	7.12(70%)	0.28(10%)	1.91
	40	532	1.44(15%)	5.34(74%)	0.3(11)	1.67
	60	490	1.61(13%)	11.6(87%)		6.34
	90	480	4.14(21%)	13.7(79)		9.12

a = fluorescence life time, b = percent contribution, c = weighted mean life time

(Upto 50%), the emission intensity is weakened and bathochromically shifted from 490 to 532 nm. The derivative **3** demonstrated a steep increase in the fluorescence with increasing water fraction from 60 to 90%, thus delivering 8 fold enhancement in emission intensity (Fig. 10b). The average life time of the derivative **3** exhibited shortening with increasing water fraction from 0% to 50% giving tri exponential fit suggesting involvement of multiple excited states and decay pathways in solvent mixture while longer life time observed in aggregates with bi-exponential fit is concomitant with increased emission intensity.

TEM images show clear morphological change from rod shaped aggregates in 60% water to spherical aggregates in 90% water (See Fig. S15 and S16, ESI). Strangely, in contrast to derivative **2**, the electron diffraction pattern both type of the aggregates (rod shaped in 60 % and spherical in 90 %) display diffraction spots, proving the crystalline nature of both. Many sharp peaks are observed in powder-XRD analysis also which confirms the semi-crystalline nature of derivative **3** in solid state (See Fig. S10, ESI). Due to the steric constrain, the derivative **3** resist complete molecular planarization and retains its twisted conformation in aggregates, thus, averting closer intermolecular donor acceptor interactions.

To find out whether the restriction of intramolecular rotation or vibrational motion of phenyl units plays any part in emission enhancement, we carried out fluorescence studies in different ratios of DMSO and glycerol (Fig. 11). Glycerol increases the viscosity of the medium, hence, restricting the rotational and vibrational motions of molecules. In lower glycerol fraction (upto 40%), emission intensity decreased with red shift in emission due to high polarity of glycerol (similar to solvent polarity effect). But as the glycerol content is further increased (upto 80%), a blue shift of emission maxima is observed (41, 52 and 74 nm for derivative **1**, **2** and **3**, respectively). Emission intensity decreased in case of derivative **1** while an increase in emission intensity was observed for **2** and **3**. Decreased emission intensity of derivative **1** even in highly viscous medium (80% glycerol) show that intramolecular phenyl vibrational and rotational motions are not involved in emission

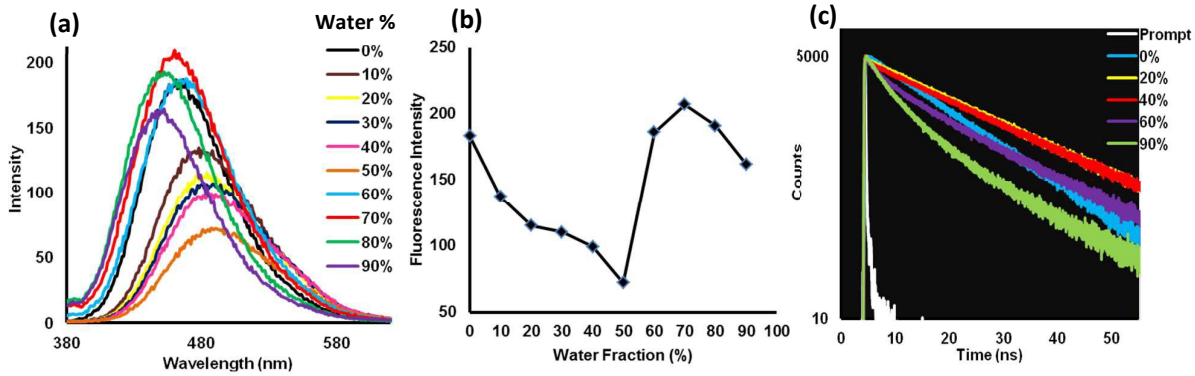

Fig. 9 Fluorescence spectra (a), fluorescence intensity (b) and time resolved spectra (c) of derivative **2** in THF with different water fractions. [slit width used – 3:1.5]

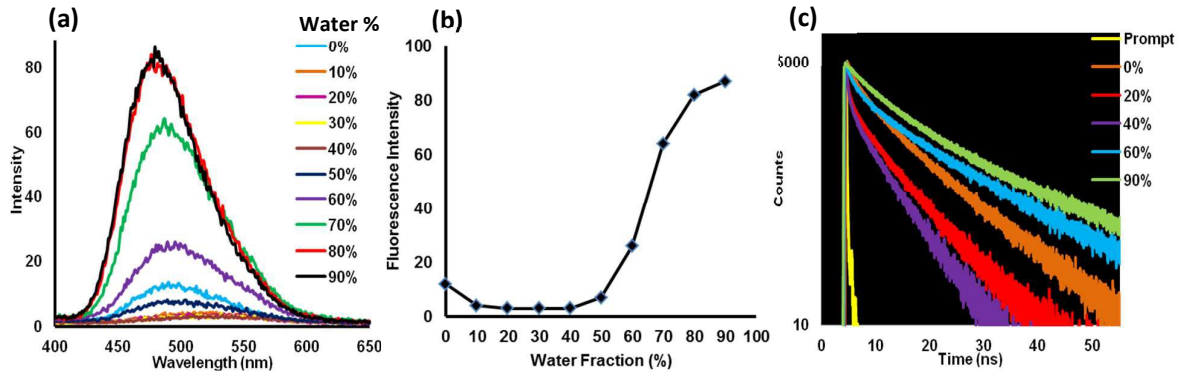

Fig. 10 Fluorescence spectra (a), fluorescence intensity (b) and time resolved spectra (c) of derivative **3** in THF with different water fractions. [slit width used – 3:1.5]

process. This may be due to the fact that the peripheral phenyl rings cannot rotate freely owing to the steric repulsion between *ortho*-hydrogens of its neighbouring phenyl groups. While the enhanced emission of derivative **2** and **3** can be explained by restriction of TICT due to very high viscosity of glycerol which restricts the torsional relaxation of molecule in excited state. We also carried out temperature dependent studies of all derivatives in 80% glycerol fraction and almost no change in emission intensity was observed on increasing temperature. These results show the absence of restriction of intramolecular rotations (RIR) in these systems. It is worth noticing that the emission spectra of derivatives **2** and **3** in 80% glycerol are similar to their thin film spectra while that of derivative **1** is 15 nm blue shifted (430 nm) as compared to its thin film (445 nm). This further supports our assumption that derivative **2** and **3** are able to prevent intermolecular donor acceptor interactions in aggregate state while in case of derivative **1** greater donor acceptor interactions are responsible for red shift and decrease in emission intensity.

From all the studies conducted above, it seems that restriction of TICT and decreased intermolecular donor-acceptor interactions due to steric effects are playing major role in maintaining efficient emission in aggregated state in case of derivative **2** and **3**. In case of derivative **1,** less sterically hindered oxadiazole acceptor group is easily approached by donor carbazole of neighboring molecule during aggregation which leads to decrease in fluorescence due to intermolecular interactions.[60-70] On the other hand, in derivative **3,** due to steric congestion near benzothiadiazole acceptor, the out of plane twisted carbazole offers great resistance to close packing of molecule in aggregate form, hence, preventing the intermolecular donor acceptor interaction which leads to emission enhancement.[73-75,20-21] Whereas derivative **2** clearly demonstrate the importance of conformational twisting and molecular packing. It shows crystalline aggregates with high luminescence in 60% water fraction indicating that the co-facial packing is well averted, hence, retaining its emission. While in 90% water fraction, decreased aggregate size force the molecules to pack tightly and become coplanar leading to stronger intermolecular donor-acceptor interactions and decrease in emission intensity.

Conclusion

In summary, a new series of a series of D-A-D molecules (**1**-**3**) with carbazole as donor while 2,5-diaryl-1,3,4-oxadiazoles, dibenzothiophene-S,S-dioxide and Benzo[1,2,5] thiadiazole as acceptors have been synthesized. Polyphenylene dendrons have also been incorporated to prevent the face to face π–π

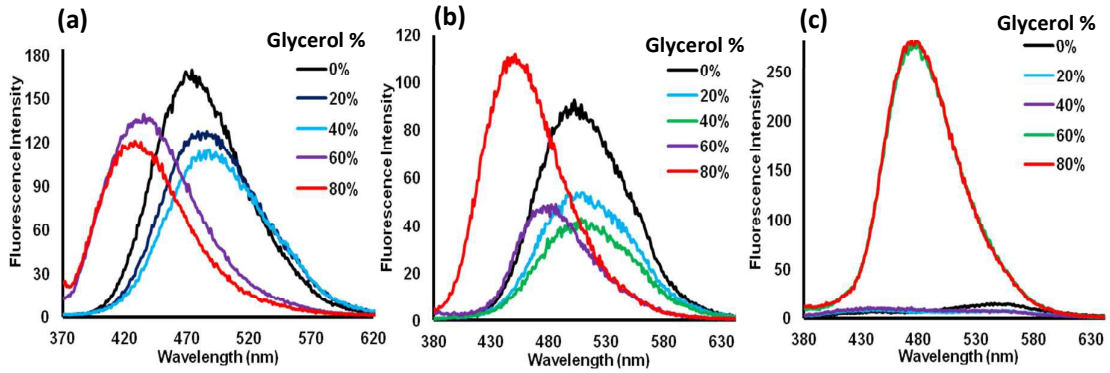

Fig. 11 Fluorescence spectra of derivative **1** (a), **2** (b) and **3** (c) in different DMSO/ glycerol ratios [conc. 10μM, slit width used – 3:1.5].

stacking in aggregates. In addition, the materials possess high thermal stability (T_d = 378-410 °C) and have relatively high band gaps (2.62-3.36 eV). Unlike traditional D–A systems, which show ACQ problem and large red shifts in solid state, these derivatives (**1**-**3**) exhibit good solid state luminescence behavior without undergoing red shift or fluorescence quenching. Despite structural similarity, these derivatives exhibited remarkably different aggregation behaviour. The present results indicate that just the combination of donors-acceptor system with bulkier dendrons is not enough to generate efficient solid state emissions but prevention of co-facial interaction of donor and acceptors in aggregates is more important. In case of derivative **3**, restriction of complete molecular planarization and steric hindrance near acceptor can effectively prevent intermolecular donor acceptor interactions, thus, leading to enhanced emission in aggregates. While in case of derivative **1**, sterically unhindered acceptor is easily approached by donor due to close molecular packing in aggregates forming weakly luminescent species. These results would be beneficial to understand the importance of minor steric effects governing the packing behaviour of molecule in aggregated state and could be helpful in designing efficient solid state emissive materials for organic electronic devices.

Acknowledgements

M. K. and V. B. are thankful to DST (ref no. SR/S1/OC-69/2012) for financial support. We are also thankful to UGC (New Delhi) for "University with Potential for Excellence" (UPE) project. G. S. is thankful to Dr. Imran A. Khan for his help in DFT calculation. G.S. is thankful to Rajiv Gandhi National Fellowship Scheme for providing fellowship.

Notes and references

1 M. Pfeiffer, S. R. Forrest, K. Leo, and M. E. Thompson, *Adv. Mater*. 2002, **14**, 1633.
2 B. D'Andrade, *Nat. Photonics* 2007, **1**, 33.
3 S. Kena Cohen, and S. R. Forrest, *Nat. Photonics.* 2010, **4**, 371.
4 T. H. Huang, J. T. Lin, L. Y. Chen, Y. T. Lin and C. C. Wu, C. *Adv. Mater*. 2006, **18**, 602.
5 S. J. Lee, J. S. Park, K. J. Yoon, Y. I. Kim, S. H. Jin, S. K. Kang, Y. S. Gal, S. Kang, J. Y. Lee, J. W. Kang, S. H. Lee, H. D. Park and J. J. Kim, *Adv. Funct. Mater*. 2008, **18**, 3922.
6 S. L. Lin, L. H. Chan, R. H. Lee, M. Y. Yen, W. J. Kuo, C. T. Chen and R. J. Jeng *Adv. Mater*. 2008, **20**, 3947.
7 M. Y. Lai, C. H. Chen, W. S. Huang, J. T. Lin, T. H. Ke, L. Y. Chen, M. H. Tsai and C. C. Wu, *Angew. Chem., Int. Ed*. 2008, **47**, 581.
8 C. H. Chen, W. S. Huang, M. Y. Lai, W. C. Tsao, J. T. Lin, Y. H. Wu, T. H. Ke, L. Y. Chen and C. C. Wu, *Adv. Funct. Mater*. 2009, **19**, 2661.
9 Y. Zhang, S. L. Lai, Q. X. Tong, M. F. Lo, T. W. Ng, M. Y. Chan, Z. C. Wen, J. He, K. S. Jeff, X. L. Tang, W. M. Liu, C. C. Ko, P. F. Wang, C. S. Lee, *Chem. Mater*. 2012, **24**, 61.
10 K. E. Linton, A. L. Fisher, C. Pearson, M. A. Fox, L. O. Palsson, M. R. Bryce and M. C. Petty, *J. Mater. Chem*. 2012, **22**, 11816.
11 Q. S. Zhang, J. Li, K. Shizu, S. P. Huang, S. Hirata, H. Miyazaki and C. Adachi, C. *J. Am. Chem. Soc*. 2012, **134**, 14706.
12 T. Nakagawa, S. Y. Ku, K. T. Wong and C. Adachi, *Chem. Commun*. 2012, **48**, 9580.
13 C. Liu, Y. Gu, Q. Fu, N. Sun, C. Zhong, D. G. Ma, J. G. Qin and C. L. Yang *Chem. Eur. J*. 2012, **18**, 13828.
14 Z. R. Grabowski, K. Rotkiewicz and W. Rettig, *Chem. Rev*. 2003, **103,** 3899.
15 Z. M. Tang, T. Lei, K. J. Jiang, Y. L. Song and J. A. Pei, *Chem. Asian J*. 2010, **5**, 1911.
16 J. A. Mikroyannidis, S. S. Sharma, Y. K. Vijay and G. D. Sharma, *ACS Appl. Mater. Interfaces* 2010, **2**, 270.
17 L. J. Huo, J. H. Hou, S. Q. Zhang, H. Y. Chen and Y. Yang, *Angew. Chem*. 2010, **122**, 1542.
18 Y. J. Cheng, S. H. Yang and C. S. Hsu, *Chem. Rev.* 2009, **109**, 5868.
19 P. T. Wu, F. S. Kim, R. D. Champion and S. A. Jenekhe, *Macromolecules* 2008, **41**, 7021.
20 B. R. Gao, H. –Y. Wang, Z.-Y. Yang, H. Wang, L. Wang, Y. Jiang, Y. W. Hao, Q. D. Chen, Y. P. Li, Y. G. Ma and H. B. Sun, *J. Phys. Chem. C* 2011, **115**, 16150.
21 B. R. Gao, H. Y. Wang, Y. W.; Hao, L. M. Fu, H. H. Fang, Y. Jiang, L. Wang, Q. D. Chen, H. Xia, L. Y. Pan, Y. G. Ma and H. B. Sun, *J. Phys. Chem. B* 2010, **114**, 128.
22 L. A. Duan, J. A. Qiao, Y. D. Sun, and Y. Qiu, *Adv. Mater*. 2011, **23**, 1137.
23 C. H. Chen, *Chem. Mater.* 2004, **16,** 4389.
24 H. Bi, K. Ye, Y. Zhao, Y. Yang, Y. Liu, and Y. Wang, *Org. Electron*. 2010, **11**, 1180.
25 X. Gong, S. Wang, D. Moses, G. C. Bazan, and A. J. Heeger, *Adv. Mater*. 2005, **17**, 2053.
26 J. D. Luo, Z. L. Xie, J. W. Y. Lam, L. Cheng, H. Y. Chen, C. F. Qiu, H. S. Kwok, X. W. Zhan, Y. Q. Liu, D. B. Zhu, and B. Z. Tang, *Chem. Commun*. 2001, 1740.
27 B. K. An, S. K. Kwon, S. D. Jung, and S. Y. Park, *J. Am. Chem. Soc*. 2002, **124**, 14410.
28 R. Hu, E. Lager, A. Aguilar-Aguilar, J. Liu, J. W. Y. Lam, H. H. Y. Sung, I. D. Williams, Y. Zhong, K. S. Wong, and E. Pena-Cabrera, *J. Phys. Chem. C* 2009, **113**, 15845.
29 W. Z. Yuan, P. Lu, S. Chen, J. W. Y. Lam, Z. Wang, Y. Liu, H. S. Kwok, Y. Ma, and B. Z. Tang, *Adv. Mater*. 2010, **22**, 2159.
30 Y. Hong, J. W. Y. Lam, and B. Z. Tang, *Chem. Soc. Rev*. 2011, **40,** 5361.
31 Z. Zhao, J. W. Y. Lam, and B. Z. Tang, *J. Mater. Chem*. 2012, **22**, 23726.
32 W. Z. Yuan, Y. Gong, S. Chen, X. Y. Shen, J. W. Y. Lam, P. Lu, Y. Lu, Z. Wang, R. Hu, and N. Xie, *Chem. Mater*. 2012, **24**, 1518.
33 W. Li, D. Liu, F. Shen, D. Ma, Z. Wang, T. Feng, Y. Xu, B. Yang, and Y. A. Ma, *Adv. Funct. Mater*. 2012, **22**, 2797.
34 L. Chen, Y. Jiang, H. Nie, R. Hu, H. S. Kwok, F. Huang, A. Qin, Z. Zhao and B. Z. Tang. *ACS Appl. Mater. Interfaces* 2014, **6**, 17215.
35 X. Y. Shen, Y. J. Wang, H. Zhang, A. Qin, J. Z. Sun and B. Z. Tang. *Chem. Commun*., 2014, **50**, 8747.
36 J. Li, Y. Jiang, J. Cheng, Y. Zhang, H. Su, J. W. Y. Lam, H. H. Y. Sung, K. S. Wong, H. S. Kwok and B. Z. Tang, *Phys. Chem. Chem. Phys*., 2015, **17**, 1134.
37 Q. Lu, X. Li, J. Li, Z. Yang, B. Xu, Z. Chi, J. Xu and Y. Zhang, *J. Mater. Chem. C* 2015, Advance Article DOI: 10.1039/C4TC02165G.
38 P. L. T. Boudreault, S. Beaupre and M. Leclerc, *Polym. Chem*., 2010, **1**, 127.
39 S. C. Lo and P. L. Burn, *Chem. Rev*., 2007, **107**, 1097.
40 A. P. Kulkarni, C. J. Tonzola, A. Babel and S. A. Jenekhe, *Chem. Mater*., 2004, **16**, 4556.
41 G. Hughes and M. R. Bryce, *J. Mater. Chem*., 2005, **15**, 94.
42 F. B. Dias, S. King, A. P. Monkman, I. I. Perepichka, M. A. Kryuchkov, I. F. Perepichka and M. R. Bryce, *J. Phys. Chem. B* 2008, **112**, 6557.

43 S. M. King, I. I. Perepichka, I. F. Perepichka, F. B. Dias, M. R. Bryce and A. P. Monkman, *Adv. Funct.Mater*. 2009, **19**, 586.
44 H. Liu, J. H. Zou, W. Yang, H. B. Wu, C. Li, B. Zhang, J. B. Peng and Y. Cao, *Chem. Mater*. 2008, **20**, 4499.
45 M. Akhtaruzzaman, N. Kamata, J. Nishida, S. Ando, H. Tada, M. Tomura and Y. Yamashita, *Chem. Commun*., 2005, 3183.
46 S. Setayesh, A. C. Grimsdale, T. Weil, V. Enkelmann, K. Mullen, F. Meghdadi, E. J. W. List, G. Leising, *J. Am. Chem. Soc*., 2001, **123**, 946.
47 M. D. Watson, A. Fechtenkotter and K. Mullen, *Chem. Rev*., 2001, **101**, 1267.
48 J. Wu, W. Pisula and K. Mullen, *Chem. Rev*., 2007, **107**, 718.
49 R. Grisorio, C. Piliego, P. Fini, P. Cosma, P. Mastrorilli, G. Gigli, G. P. Suranna and C. F. Nobile, *J. Phys. Chem. C*, 2008, **112**, 7005.
50 D. C. Shin, J. H. Ahn, Y. H. Kim and S. K. Kwon, *J. Polym. Sci.: Part A: Polymer Chemistry*, 2000, **38**, 3086.
51 C. R. Newmoyer and E. D. Amstutz, *J. Am. Chem. Soc*. 1947, **69**, 1920.
52 J. F. Ambroso and R. F. Nelson, *J. Electrochem. Soc*. 1968, **115**, 1159.
53 J. Pommerehne, H. Vestweber, W. Gusws, R. F. Mahrt, H. Bassler, M. Porsch and J. Daub, *Adv. Mater*., 1995, **7**, 55.
54 Y. Zhou, Q. G. He, Y. Yang, H. Z. Zhong, C. He, G. Y. Sang, W. Liu, C. H. Yang, F. L. Bai and Y. F. Li, *Adv. Funct. Mater*. 2008, **18**, 3299.
55 N. Prachumrak, S. Pojanasopa, R. Tarsang, S. Namuangruk, S. Jungsuttiwong, T. Keawin, T. Sudyoadsukb and V. Promarak, *New J. Chem*., 2014, **38**, 3282.
56 C. H. Zhao, Y. H. Zhao, H. Pan, G. L. Fu, *Chem. Commun*. 2011, **47**, 5518.
57 M. Shimizu, Y. Takeda, M. Higashi and T. Hiyama, T. *Angew. Chem*. 2009, 121, 3707.
58 C. H. Zhao, A. Wakamiya, Y. Inukai and S. Yamaguchi, *J. Am. Chem. Soc*. 2006, **128**, 15934.
59 H. Inomata, K. Goushi, T. Masuko, T. Konno, T. Imai, H. Sasabe, J. J. Brown and C. Adachi, *Chem. Mater*. 2004, **16**, 1285.
60 J. Mei, Y. Hong, J. W. Y. Lam, A. Qin, Y. Tang and B. Z. Tang, *Adv. Mater*. 2014, **26**, 5429.
61 S. Kim, Q. Zheng, G. He, D. J. Bharali, H. E. Pudavar, A. Baev and P. N. Prasad, *Adv. Funct. Mater*. 2006, **16**, 2317.
62 Z. Q. Yan, Z. Y. Yang, H. Wang, A. W. Li, L. P. Wang, H. Yang and B. R. Gao, *Spectrochim. Acta A: Mol. Biomol. Spectr*. 2011, **78**, 1640.
63 H. H. Fang, Q. D. Chen, J. Yang, H. Xia, B. R. Gao, J. Feng, Y.G. Ma and H. B. Sun, *J. Phys. Chem. C* 2010, **114**, 11958.
64 W. Qin, D. Ding, J. Liu, W. Z. Yuan, Y. Hu, B. Liu and B. Z. Tang. *Adv. Funct. Mater*. 2012, **22**, 771.
65 A. Kawski, B. Kuklinski and P. Bojarski, *Chem. Phys. Lett*. 2008, **455**, 52.
66 A. Marini, A. Munoz-Losa, A. Biancardi, B. Mennucci, *J. Phys. Chem. B* 2010, **114**, 17128.
67 H. Auweter, H. Haberkorn, W. Heckmann, D. Horn, E. Lüddecke, J. Rieger and H. Weiss, *Angew. Chem. Int. Ed*. 1999, **38**, 2188.
68 Y. Zhang, J. Sun, G. Bian, Y. Chen, M. Ouyang, B. Hua and C. Zhang. *Photochem. Photobiol. Sci*., 2012, **11,** 1414.
69 D. Setiawan, A. Kazaryan, M. A. Martoprawiro and M. Filatov, *Phys. Chem. Chem. Phys*. 2010, **12**, 11238.
70 L. Skardziute, K. Kazlauskas, J. Dodonova, J. Bucevicius, S. Tumkevicius and S. Jursenas, *Tetrahedron* 2013, 9566.
71 Y. Ren, J. W. Y. Lam, Y. Dong, B. Z. Tang and K. S. Wong, *J. Phys. Chem. B*, 2005, **109**, 1135.
72 M. Yang, D. Xu, W. Xi, L. Wang, J. Zheng, J. Huang, J. Zhang, H. Zhou, J. Wu and Y. Tian. *J. Org. Chem*. 2013, **78**, 10344.
73 S. S. Palayangoda, X. Cai, R. M. Adhikari and D. C. Neckers, *Org. Lett*. 2008, **10**, 281.
74 Y. Liu, X. Tao, F. Wang, X. Dang, D. Zou, Y. Ren and M. Jiang, *J. Phys. Chem. C* 2008, **112**, 3975.
75 J. Xu, X. Liu, J. Lu, M. Zhu, C. Huang, W. Zhou, X. Yin, H. Liu, Y. Li and J. Ye, *Langmuir* 2008, **24**, 4231.